International Congress of Science and Technology of Metallurgy and Materials, SAM - CONAMET 2013

Structural Evolution of Pearlite in Steels with Different Carbon Content under Drastic Deformation during Cold Drawing

E. Brandaleze*

Metallurgical Department, Universidad Tecnológica Nacional, Colón 332, San Nicolás 2900, Argentina

Abstract

Steel wires, under severe cold drawing deformation, develop high strength. High carbon steel (C>0.80%) has a great demand in the steel market because of the extremely high strength (5-6 GPa). For this reason it is relevant to increase the knowledge on the structural evolution and deformation mechanisms involved during wiredrawing process due to their critical applications, among which we can mention wires for: bridges, cranes and tire cord. The mechanical behaviour aptitude is determined by torsion test. When the fracture surface is flat, the wire is apt. On the opposite, an irregular fracture surface (delamination) means poor mechanical properties.

This paper presents a comparative study on steel wires with different carbon contents (0.40% C and 0.80% C) in order to compare the structural evolution at high deformation and to verify the impact of carbon content on the pearlite deformation and cementite stability. Samples tested under torsion with and without delamination problems, were selected. The microstructural study was carried out applying light and scanning electron microscopy (SEM). Finally, the structural information was correlated with results of differential scanning calorimetry (DSC) and thermodynamic properties obtained by Fact Sage simulation.

The structural study verified the presence of curling phenomenon in both steels grades, with different carbon content. The effect of the ferrite on deformation mechanisms during wiredrawing was clearly visualized. It was possible to verify differences (~ 26%) in the interlaminar spacing (λ) of the pearlite between wires that present normal and delaminated behaviour under torsion test. The ductility loss (in the delaminated wire) is promoted by multiple causes: higher interlaminar spacing, high nitrogen content in the product and the presence of dynamic strain aging, which is promoted by cementite destabilization and the formation of ε carbide.

Published by Elsevier Ltd. This is an open access article under the CC BY-NC-ND license
(http://creativecommons.org/licenses/by-nc-nd/4.0/).
Selection and peer-review under responsibility of the scientific committee of SAM - CONAMET 2013

Keywords: high strength; pearlitic steels; wires; structure; cold drawing

* E. Brandaleze. Tel.: 54-336-4420830; fax: 54-336-4420820
 E-mail address: ebrandaleze@frsn.utn.edu.ar

1. Introduction

Severely plastically deformed steels have great technological importance as high-strength materials. Nematollahi et al. (2013) and Li (2012) mentioned that heavily cold drawn pearlitic steels exhibit the highest tensile strength (5-6 GPa) of any material known to date. Despite numerous experimental and theoretical investigations, the mechanisms of the extraordinary strength are not yet fully understood. The special properties of the pearlitic steel wires (C>0.80%) allow us to use them in critical applications such as wires for: bridges, cranes, tire cords among others.

It is known that during plastic deformation, a small fraction of the mechanical energy is stored in the metal, mostly in the form of dislocations. Hughes et al. (2003) described that dislocations are not randomly distributed, are organized themselves into mosaic patterns. In general, this occurs near 2D edges surrounded by regions with few dislocations, resulting in a misorientation which can reach 15º at very high strain conditions. The mosaic pattern subdivides the original grains during deformation. The main factors that affect the dislocation movements are:

- Stacking fault energy (SFE) that modifies the ability of a dislocation to glide onto an intersecting slip plane (cross slip). The 3D mobility increases with increasing SFE.
- Friction stress or Peierls-Nabarro force is the lattice resistance to dislocation slip. This force is small in face-centered-cubic (fcc) and larger in the body-centered-cubic (bcc) materials.
- Atoms of solutes or impurities that interact strongly with the gliding dislocations, increase the friction stress.
- The solutes favor the planar glide. Also they promote that dislocations move following one to each other on exactly the same sliding plane.
- Temperature, in the case of thermally activated glide of dislocations.
- Strain rate.
- Deformation mode and grain orientation, determine the slip system activity. The slip pattern is thus determined by the degree of activation of different slip systems.
- Strain percentage. At large strain, the shape of cell blocks (or mosaics) is planar for: rolling, compression, torsion and simple shear. However, it is cylindrical in cold drawn and extruded products. For large strains (99.5%), a considerable structure refinement grade can be achieved including nanoscale changes that promote very high resistances. The resulting texture in fcc metal would be <111> + <110>. If the material is bcc the texture is <110>.

Cold drawn metals and other types of alloys present a structural phenomenon named"curling". This structural aspect has been observed in Cu-Fe alloys, Cu-Nb and heavily cold drawn steel, see Bolmaro et al. (2005) and Brandaleze et al. (2012). In pearlitic steels, the wiredrawing promotes thinning of the cementite and ferrite lamellaes, metallographic and crystallographic texture changes and also variations in the interlamellar interface nature, Brandaleze et al. (2012). Fully pearlitic steels (C> 0.80%) also could present localized plastic deformation and dynamic strain aging.

This paper presents a comparative study between two steel grades (0.40% C and 0.84% C) with the aim toincrease the knowledge of deformation mechanisms that can affect the mechanical behavior of these cold drawn materials.

In order to understand the origin of delamination under torsion test conditions, a structural characterization of steel (0.84% C) samples was carried out. Normal and delaminated wire samples were characterized by light and electron scanning microscope (SEM). The interlamellar spacing was determined by SEM. The information is correlated with differential scanning calorimetry (DSC) results up to 600 °C to determine the presence of dynamic strain aging phenomenon.

2. Experimental

The study was carried out on wires of two different steel grades: A1 (0.40%C) and A2 (0.84%C). One of the main objectives was to increase the knowledge on the deformation mechanisms developed during wiredrawing. The samples corresponding to the steel A2 (0.84%C), include wires that suffer delamination (A2D) and other that present a normal behavior (A2N), during the torsion test. All the samples studied correspond to wires cold drawn and heat treated under the same operation conditions. The reduction considered was from 9.05 mm to 3.25 mm. The A2D wire present slow mechanical resistance (109 daN/mm^2) respect to the limit established by the technical

qualification of this type of product (110 daN/mm^2). Also the N content is high (70 ppm) considering the maximum value permitted for high carbon wires is 80 ppm.

Longitudinal and transverse wire samples were prepared for the structural study. The observation of the structure was carried out by an Olympus GX51 microscope with the image analysis system Leco IA 32. The pearlite interlamellar space (λ) was measured by a scanning electron microscope FEI Quanta 200.

In order to verify the presence of dynamic strain aging at low temperatures, differential scanning calorimetry (DSC) tests were developed using a Shimadzu DTA60 instrument. The tests include different heating rates (5ºC/min and 25ºC/min) up to 600ºC. Finally, thermodynamic properties of Fe$_3$C, Fe$_{2.5}$C and FeC were estimated by Fact Sage simulation.

3. Results and Discussion

3.1. Structure Study

In order to evaluate different structural aspect between the wires of both steel grades, samples with nital etching were observed by light microscopy. A1 sample (0.40%C) shows a ferritic-pearlitic structure. However, the samples with 0.84 %C (A2N and A2D) present a fully pearlitic structure. The results were corroborated by electron scanning microscopy (SEM), see Fig. 1 and 2.
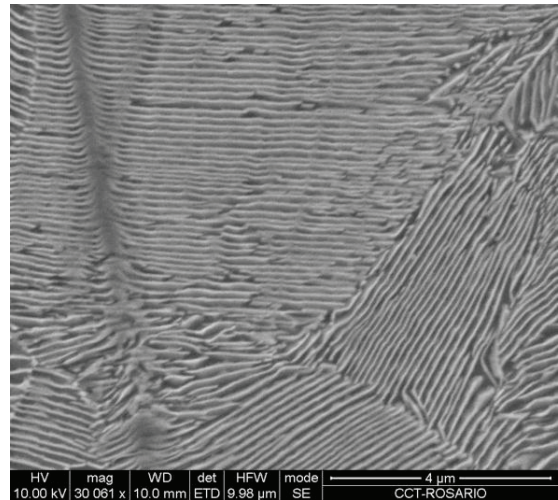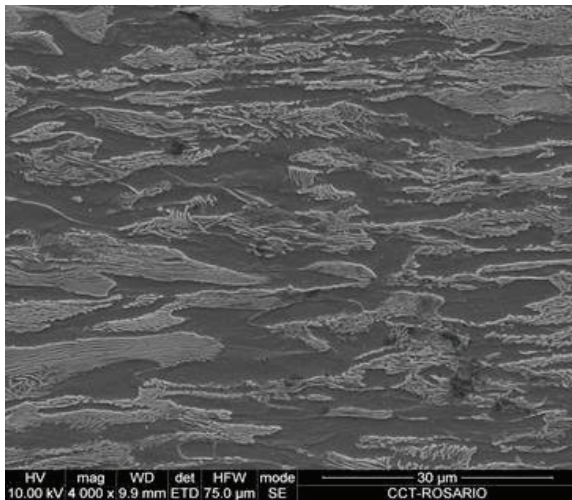
Fig. 1. Ferritic-pearlitic structure corresponding to A1 (0.40%C) sample.   Fig. 2. Fully pearlitic structure corresponding to A2 (0.84%C) sample.

The curling effect caused during wiredrawing was identified in both steel grades (A1 and A2) with different carbon content and microstructure characteristics. Nevertheless, the effect is more enhanced in the fully pearlitic wire A2. Clearly the ferritic-pearlitic structure that also presents curly behavior, shows the impact of ferrite content on the structural evolution under wiredrawing deformation, see Fig. 3 and 4.

The curling phenomenon is caused by a pearlite colonies reorientation mechanism that is related to: the sliding mechanism of dislocations, localized shear and the pearlite grains rotation around wire axis (see figure 5). Kumar et al (2011), describe the phenomenon such as the bending and kinking of pearlite colonies around the wire axis. As a consequence a fiber texture [110] is developed. This texture was checked by X-ray diffraction in a previous paper, Brandaleze et al. (2012).

Under uniaxial tensile test, pearlite colonies which present interlamellar spacing λ_0 and Miller indexes h_0, k_0 y l_0, change to a new orientation (radial [001]) around the wire axis and also a thinner interlaminar space in coincidence

with the observations described by Zelin et al. (2002). The lowest pearlite content in the A1 wire decreases the curling effect and the interlamellar thinning because of ferrite phase proportion and ductility, see Fig.3. The interlamellar spacing could be interpreted by ec. (1):

$$\lambda = \lambda_0 \exp(-k\varepsilon/2) \tag{1}$$

Where λ is the interlamellar spacing, λ_0 is the initial interlamellar spacing, $k=1$ is the constant value for wiredrawing and ε is the deformation.
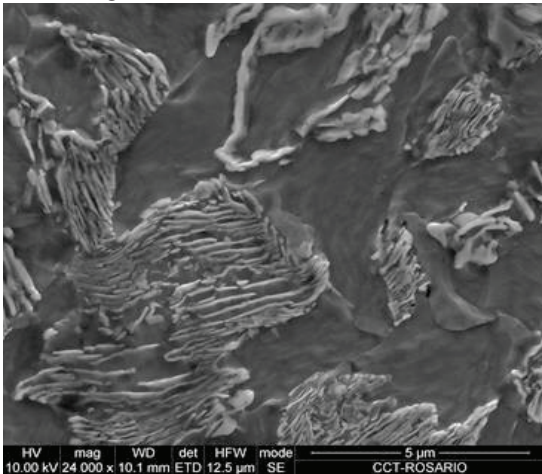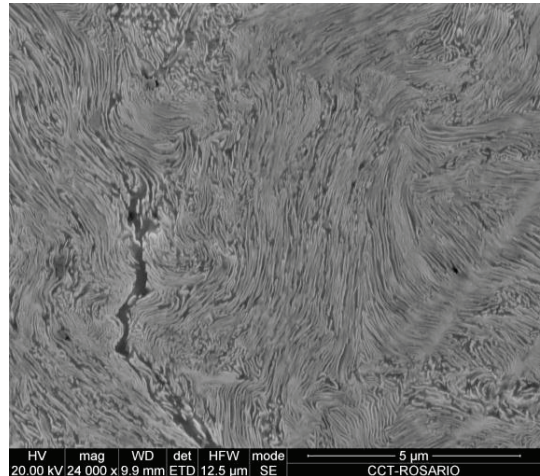

Fig. 3. Curling effect present in the sample A1.

Fig. 4. Curling effect present in the sample A2.

Fig. 5.Pearlite colonies rotation around the steel wire axis.

The interlamellar spacing and cementite lamellar thickness was measured on transverse samples of the steel A2 (A2N and A2D) by electron scanning microscopy (SEM). The measurements were carried out on two zones of the wire section (center and periphery). Figure 6 shows that the interlamellar spacing in the center zone of both wires is lower than in the periphery zone.
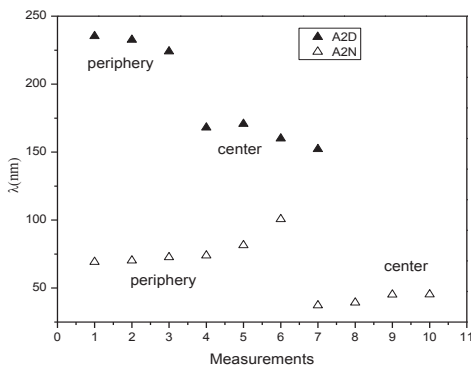

Fig. 6. Interlamellar spacing values obtained on transverse samples of normal (A2N) and delaminated (A2D) wires
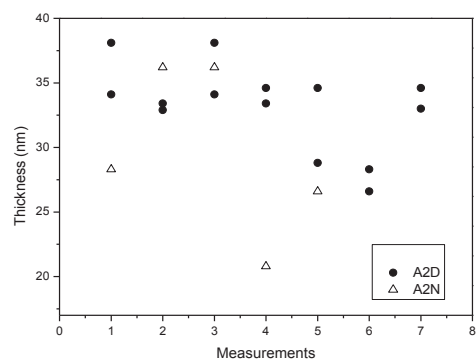

Fig. 7. Cementite (Fe₃C) lamellas thickness values obtained on transverse samples of normal (A2N) and delaminated (A2D) wires

In sample A2D the interlamellar spacing in the center is ~ 33 % lower than in the periphery. In the case of A2N wire the difference between the center and the periphery of the sample is about 34 %. The greatest degree of interlamellar spacing reduction is located into the center of both wires. Considering the central zone of the wires, that is the place in which the delamination crack propagation begins, it is possible to verify that the interlamellar spacing present in A2N (with normal behaviour) is 26% lower than the corresponding values of A2D. The results corroborate the higher ductility of the A2N wire under torsion and are consistent with the lower mechanical resistance of the wire A2D verified under torsion test (109 daN/mm^2). It is important to mention that the product requirement is110 daN/mm^2. Another factor of importance is the high content of N (70 ppm).

The thicknesses of cementite (Fe$_3$C) lamellas are quite similar in both materials (30 to 35 nm). Cottrell (1993) describe the cementite crystal structure as a local coordination of metal atoms around a carbon atom forming an approximately trigonal prismatic cell with the carbon atom in the central, interstitial position. The lattice parameter of the cementite is 4.5 Å, for this reason it is possible to think in a lamella thickness of ~ 120 atoms. With thickness about 100 nm, cementite becomes highly plastic, Zelin et al. (2002). On this base it is possible to think that cementite in both steel wires (A2N y A2D) are at this plasticity condition. At higher magnification (>100000x) cementite globulization and fragmentation was visualized in the center of both wire samples. The spherical particles are 48 nm in diameter. It was observed that cementite fragmentation is enhanced in A2D wire. Bae C.H. (1996) confirms that this structural change could promote microcracks propagation from the center of the wire under deformation, promoting delamination under torsion test (Fig. 8).
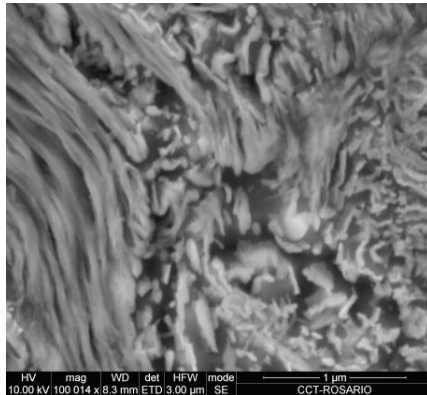

Fig. 8. Central zone of the A2N steel wire with presence of globulization and fragmentation of cementite.

Also, cementite lamellas present fibers due to intensive cold deformation. The fiber diameter is around 28 nm (~ 112 atoms). The quantity of fibers is considerable high in the wire with normal behaviour (A2N), see Figs. 9 and 10.
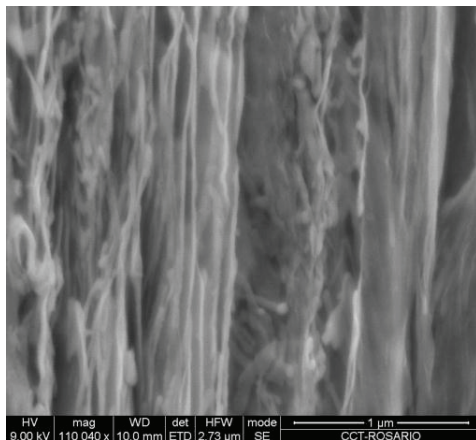

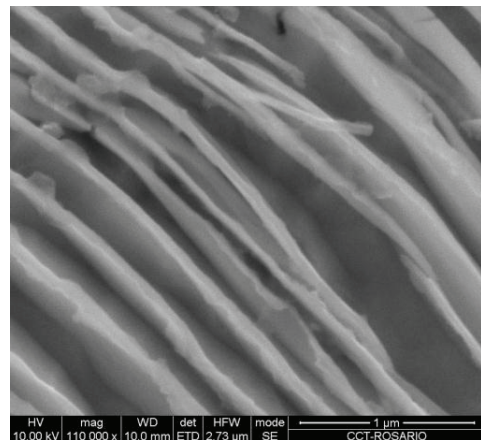Fig. 9. Presence of fibers in pearlite (sample A2N).

Fig. 10. Pearlite and fibers in sample A2D.

Based on the above descriptions it is possible to consider a change in the nature of the ferrite-cementite interface. Zelin (2002), comment that Van Acker has measured by neutron diffraction the stresses in the interface and resulting in a very high value (2000 MPa). As a consequence the interface may promote the carbon drag from the cementite to the ferrite interface. This phenomenon promotes cementite dissolution transformation as a consequence the probable precipitation of ε carbide ($Fe_{2.5}C$) in the interface, the increase of carbon content in the ferrite and the migration of them to dislocations. Cottrell (1993), explained that the cementite present a trigonal structure with the atom of carbon placed in the central interstitial site and it could have a transformation to others type of carbides in which the carbon atom moves to octahedral sites. Gavrijuk (2001) and Kumar (2011) confirm that when the reduction of interlamellar spacing during deformation is important, more pronounced cementite dissolution exists. Also, the increase of interfacial area between ferrite and cementite lamellas and the adiabatic heat produced during wiredrawing enhanced the cementite dissolution and transformation. The temperature during wiredrawing could reach 150ºC or 200ºC. Both facts promote dynamic strain aging and modify the mechanical resistance increasing up to ~ 5 %. Nematollahi et al. (2013) also propose that carbon atoms can either segregate to microstructural defects, such as dislocations/grain boundaries or dissolve in ferrite matrix. By atom probe measurements the author determined that carbon content in ferrite increase up to ~ 1 at. %. Min et al. (2010), suggested that a larger binding energy between carbon atoms and dislocations in ferrite than the attraction energy between carbon and cementite makes the carbon drag possible from cementite, by the dislocations. Gavrijuk (2001) and Min (2010) also discusses the cementite dissolution phenomena due to cold work of pearlitic steel based on experimental data obtained using Mössbauer spectroscopy and internal friction. The author inform that the enthalpy of binding between carbon atoms and dislocations in ferrite is ~ 0.8 eV according to the internal friction measurements and it varies from 0.2 to 1.8 eV if the ferrite contains different alloys elements. Also, it is necessary to consider the energy of the Fe-C binding. During wiredrawing dislocations in the ferrite-cementite interface can absorb more than 20 carbon atoms/atomic plane, along the dislocation line. Summing up, the strong interaction of carbon atoms with dislocations is the more reliable reason for cementite dissolution, or more precisely speaking the cementite destabilization due to Gibbs-Thomson effect. The results obtained for both steels A1 (0.40%C) and A2 (0.84%C), demostrate that lower carbon content in the steel (or higher content of ferrite in the structure) inhibits the interlamellar spacing reduction during wiredrawing and in consequence carbon atoms drag is considerable low despite the curling effect in the structure and the fiber texture [110] present in the wires.

3.2. Differential scanning calorimetry (DSC)

In order to verify the presence of a dynamic strain aging phenomenon at lower temperatures, differential scanning calorimetry tests were carried out up to 600ºC on both samples A2N and A2D. The results demonstrate that the material A2D present a greater heat liberation in the range between T=150ºC - 250ºC, respect to the sample A2N(Fig. 11).
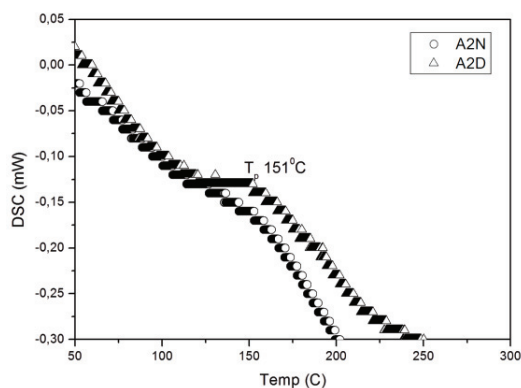

Fig. 11. DSC curves of A2N and A2D wires analyzed between 50 ºC and 250ºC.

Zelin (2002) interpreted this transformation such as the ε carbide formation. Nematollahi et al. (2013) explained that at this temperature the carbon migration to the dislocations core is produced. On this base, it is possible to suppose that the higher ε carbide formation in the A2D wire permits to think in a more important dynamic strain aging effect respect to the A2N material. The ε carbide promotes a pinning effect on dislocations and this mechanism (dynamic strain aging) together with the high free N content, the globulization and fragmentation of cementite in the center zone of the wire, probably causes the mechanical properties decrease and delamination of A2D wire.

Other manner to verify those suppositions is by a thermodynamic stability analysis of iron carbides at lower temperatures applying the Fact Sage software. Free energy values (G^0) of Fe_3C (cementite), $Fe_{2.5}C$ (ε carbide) and FeC (iron carbide), were determined. The results obtained show that at low temperature if cementite become unstable by deformation during wiredrawing conditions, the $Fe_{2.5}C$ (ε carbide) is the more probable to precipitate (Fig. 12).
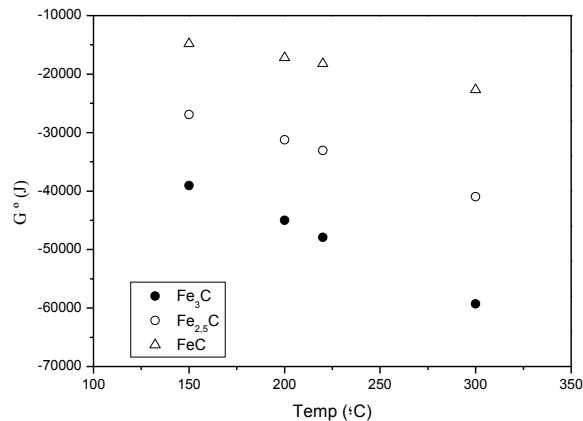

Fig. 12. Thermodynamic stabilities of iron carbides estimated by Fact Sage.

4. Conclusions

On the base of the results it is possible to conclude that:

- Both steels A1 (0.40%C) and A2 (0.80%C) present curling effect under wiredrawing process. The effect is visualized on transverse samples. The influence of ferrite content as inhibitor of the reduction of interlamellar spacing was clearly identified in A1 wire.
- In both A2 (0.80%C) wires, for a diameter reduction of 9.05 mm to 3.25 mm, the interlamellar spacing (λ) present a considerable decrease. In the normal wire (A2N), λ~ 26%, is considerable lower than the delaminated wire A2D in which λ~ 34%. This could partially justify the better ductility of A2N wire and adequate mechanical properties respect to A2D.
- The thickness of cementite lamellas measured by scanning electron microscopy (about 30 – 35 nm) permits to predict that they present ~ 120 atoms of width indicating that are highly plastic.
- By differential scanning calorimetry (DSC) the dynamic strain aging phenomenon presence in both wires was determined. Nevertheless in A2D wire, the dynamic strain aging was more important than in A2N and this behaviour is associated to: the high N content and the presence of cementite globulization or fragmentation in the center of the wire. Both effects promote delamination and degradation of the mechanical properties under torsion test.

- By Fact Sage application, it is possible to confirm the possibility of the Fe_3C to $Fe_{2.5}C$ transformation at low temperatures (150ºC-300ºC). These temperatures could be reached during wiredrawing because of the heat liberation, promoting the dynamic strain aging.
- The study permits to explain the structural effects on the extraordinary mechanical resistance developed by wires of 0.84 %C during wiredrawing process.

Acknowledgements

References

Cottrell A.H., 1993, A theory of cementite, Materials Science and Technology, 9, 277- 280.

Bae C. M., Nam W.J., Lee C.S., 1996, Effect of interlamellar spacing on the delamination of pearlitic steel wires, Scripta Materialia, 35, 5, 641-646.

Bolmaro, R. E., Fourty, A., Signorelli, J. W. and Brokmeier, H.G., 2005. Development of wire drawing textures in Cu-Fe: the influence of macroscopic and microscopic heterogeneities, Modeling Simul. Mater. Sci. Eng. 13, 1-19.

Brandaleze, E, Tormo, J., Cabanillas, M., 2012, Study on the delamination defect caused during torsion test on high carbon steel wires, 3th Mechanical Eng. Argentan Congress, III CAIM 2012, G, 340-350.

Gavriljuk, V.G., (2001), Comment on "Effect of interlamellar spacing on cementite dissolution during wire drawing of pearlitic steel wires", Scripta Materialia, 45, 1469-1472.

Hughes, S.A., Hansen, N., 2004. Plastic deformation structures, Metallography and Microstructures, in "ASM Handbook" 9, (Ed.). ASM International, 193-214.

Kumar P., Gurao N.P., Haldar A., Suwas S., (2011), Progressive changes in the microstructure and texture in pearlitic steel during wire drawing, ISIJ International, 51, 4, 679-684.

Li, Y.J., Choi, P., Goto, S., Borchers, C., Raabe, D., Kirchheim, R., (2012), Evolution of strength and microstructure during annealing of heavily cold drawn 6.3 GPa hypereutectoid pearlitic steel wire, Acta Materialia, 60, 4005-4016.

Min, N., Li, W., Li, H., Jin, X., (2010) Atom probe and Mössbauer spectroscopy investigations of cementite dissolution in a cold drawn eutectoid steel, J. Mater. Sci. Technol., 26, 776-782.

Nematollahi, G.A., Von Pezold, J., Raabe, D., 2013. Thermodynamics of carbon solubility in ferrite and vacancy formation in cementite in strained pearlite, Acta Materialia 61,1773-1784.

Zelin, M., 2002, Microstructure evolution in pearlitic steels during wire drawing, Acta Materialia, 50, 4431-4447.